Materials and Structures (2016) 49:45–55
DOI 10.1617/s11527-014-0473-6

ORIGINAL ARTICLE

The use of fractional calculus to model the experimental creep-recovery behavior of modified bituminous binders

Alberto Sapora · Pietro Cornetti · Alberto Carpinteri · Orazio Baglieri · Ezio Santagata

Received: 17 July 2014 / Accepted: 13 November 2014 / Published online: 27 November 2014

Abstract Fitting of experimental creep-recovery curves obtained from rheological tests carried out on viscoelastic materials can reveal difficulties when handled by classical rheological theories, which generally provide exponential-type functions requiring a great number of parameters to be determined. Fractional calculus may represent a natural framework to develop more synthetic and efficient methods, overcoming most of the problems encountered with the classical approach. In this paper, a fractional model consisting of a dashpot in series with a springpot is proposed to describe the viscoelastic behavior of modified bituminous binders used in road pavements. The purpose is twofold: (i) to evaluate the adequacy of a rheological model involving a limited number of parameters, each of which with a precise physical meaning; (ii) to improve the accuracy of other fractional approaches proposed in literature. The investigation was validated by means of experimental data gathered from shear creep-recovery tests carried out at various temperatures on two modified bituminous binders containing a styrene–butadiene–styrene polymer and crumb rubber from end-of-life tires.

Keywords Viscoelasticity · Creep-recovery tests · Bituminous binders · Fractional calculus

A. Sapora (✉) · P. Cornetti · A. Carpinteri
Department of Structural, Geotechnical and Building Engineering, Politecnico di Torino, Corso Duca degli Abruzzi 24, 10129 Turin, Italy
e-mail: alberto.sapora@polito.it

O. Baglieri · E. Santagata
Department of Environment, Land and Infrastructure Engineering, Politecnico di Torino, Corso Duca degli Abruzzi 24, 10129 Turin, Italy

1 Introduction

The property of a body, when deformed, to exhibit both an elastic and a viscous behavior as a result of the simultaneous storage and dissipation of mechanical energy is known as viscoelasticity. In other terms, viscoelastic materials are those for which the stress–strain constitutive relationship depends upon time. Indeed, this framework represents the research field where fractional calculus, i.e. the mathematical branch dealing with derivatives and integrals of arbitrary orders [35, 37], has been mostly applied. The reason is related to the fact that many viscoelastic materials show a creep/relaxation behavior of the power-law type [13, 14, 22, 23, 31, 32], while classical rheological models used to describe such a response generally rely on exponential-type functions. As a consequence, a huge number of elements (and thus of parameters) have to be taken into account in order to approximate a power-law expression, giving rise to several drawbacks: (i) it is not always possible to provide a clear mechanical meaning to all coefficients; (ii) the

numerical procedure employed to fit the parameters is not trivial, these being subjected to several physical constraints [45, 46]. On the contrary, power-law expressions are naturally generated by assuming a constitutive law of the fractional type, i.e. involving non-integer order derivatives of stress and/or strain [44]. Moreover, it should be pointed out that fractional operators have a simple definition in terms of Laplace transforms, so it is not difficult to obtain the relaxation modulus starting from creep compliance (and vice-versa), being these functions strictly related in the Laplace domain (e.g. [24]).

A detailed list of references on fractional applications to viscoelasticity can be found in [8, 21, 24], while significant contributions which are relevant in the context of this paper are the following: the pioneering work by Caputo and Mainardi [7] on dissipation in anelastic solids; the application to problems in polymer physics and rheology discussed in [14]; the studies on concrete structures carried out in [4, 5]; the applications to bioengineering reported in [22]; the approach proposed in [27] to simulate the surface wave response of soft tissue-like materials; the analytical investigation of wave propagation in a viscoelastic rod of finite length carried out in [1, 2]; the analysis of the behavior of different elastomers [12]; the finite element (FE) implementation presented in [30].

Only few studies focused on bituminous materials used for road pavements. The first attempt, to the authors' best knowledge, is due to Oeser et al. [33], who employed the fractional Burger element to describe creep-recovery curves of bituminous mixtures. Both the cases of a constant fractional order α and of an exponent α varying with strain (i.e., with time) were discussed. The constitutive law was implemented through a non-linear computational model in the spirit of the FE method. More recently, Celauro et al. [9] proposed the simple two-coefficient fractional dashpot (also known as Scott-Blair element or springpot) to analytically obtain loading and unloading curves which were compared to experimental data derived from creep-recovery tests performed on bituminous mixtures. Although promising, this last study presents significant points of weakness. First of all, discrepancies with experimental data were observed for tests involving long loading times and additional parameters were hence introduced, thus leading to a four-parameter model. From a physical point of view, this choice may be questionable. Secondly, according to the springpot element (and, more in general, to all "pure" fractional models as observed in [33]), recovery strains tend to zero for infinite times, whereas a permanent viscous strain is experimentally observed in the case of bituminous materials.

With the purpose of overcoming these drawbacks and of giving an original contribution to research on bituminous binders, a three-parameter model consisting of a springpot in series with a dashpot was considered in the investigation described in this paper (see also [11]). The model was applied to creep-recovery test results obtained at different temperatures for two modified bituminous binders. The paper is organized as follows: classical rheological models are presented in Sect. 2, while basic fractional approaches are discussed in Sects. 3 and 4 includes a description of the performed experimental investigation, an illustration of the procedure adopted to fit model parameters, the comparison between test data and theoretical results; finally, Sect. 5 contains the main conclusions of the study.

2 Classical rheological models

Elastic behavior is generally modeled by a one-dimensional Hookean spring, whose stress–strain ($\sigma - \varepsilon$) constitutive relationship, as a function of time t, is written as:

$$\sigma(t) = E\varepsilon(t) \tag{1}$$

being E the spring stiffness.

Fluid viscous response is described by a dashpot element, whose constitutive law is:

$$\sigma(t) = \eta \frac{d\varepsilon(t)}{dt} \tag{2}$$

where η is dynamic viscosity.

Viscoelastic materials exhibit both elastic and viscous behaviors, which are then modeled by properly combining springs and dashpots.

In the first part of the analysis presented in this paper, the viscoelastic constitutive equation is expressed by using a creep-based formulation of the following type:

$$\varepsilon(t) = D(t)\sigma_0 \tag{3}$$

being σ_0 the applied stress and $D(t)$ the creep compliance function, which for the spring is simply $D = 1/E$ and for the dashpot takes the form $D(t) = t/\eta$.

2.1 Maxwell and Kelvin–Voigt models

The Maxwell model consists of a spring and a dashpot in series (Fig. 1a). The two elements are subjected to the same stress, while total strain is given by the sum of the contributions of the spring and of the dashpot. Thus, it is not difficult to obtain the constitutive relationship by differentiating Eq. (1) and by adding the result to Eq. (2):

$$\sigma(t) + \frac{\eta}{E}\frac{\mathrm{d}\sigma(t)}{\mathrm{d}t} = \eta\frac{\mathrm{d}\varepsilon(t)}{\mathrm{d}t} \tag{4}$$

The Kelvin–Voigt model is obtained by combining in parallel a spring and a dashpot (Fig. 1b). In this case the two elements are subjected to the same strain, whereas total stress is the sum of two terms associated to the component models. The constitutive law can be achieved by adding Eq. (1) to Eq. (2), leading to:

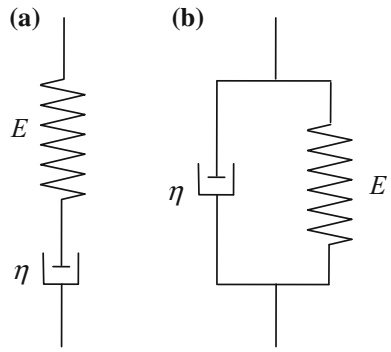

Fig. 1 Maxwell model (**a**); Kelvin–Voigt model (**b**)

$$\sigma(t) = E\varepsilon(t) + \eta\frac{\mathrm{d}\varepsilon(t)}{\mathrm{d}t} \tag{5}$$

In the case of the Maxwell model, creep compliance $D(t)$ is:

$$D(t) = \frac{1}{E} + \frac{t}{\eta}, \tag{6}$$

while for the Kelvin–Voigt model it is represented by an exponential-decaying function of the following type:

$$D(t) = \frac{1}{E}[1 - \exp(-t/\bar{t})] \tag{7}$$

where $\bar{t} = \eta/E$ is known as retardation time.

2.2 Generalized models

Since both models introduced in the previous section have only two parameters, their capability of representing the behavior of complex materials is limited. However, they can be combined in several ways, thus leading to more versatile and useful generalized models (the reader is referred to [46] for a complete description).

Typical examples of such models are: (i) the four-parameter Burger model (Fig. 2a), which is obtained by arranging in series a Maxwell element with a Kelvin–Voigt element; (ii) the $2n$-parameter generalized Kelvin–Voigt model (Fig. 2b), achieved by considering n Kelvin–Voigt elements in series with an isolated spring. In this last case, the creep compliance function is:

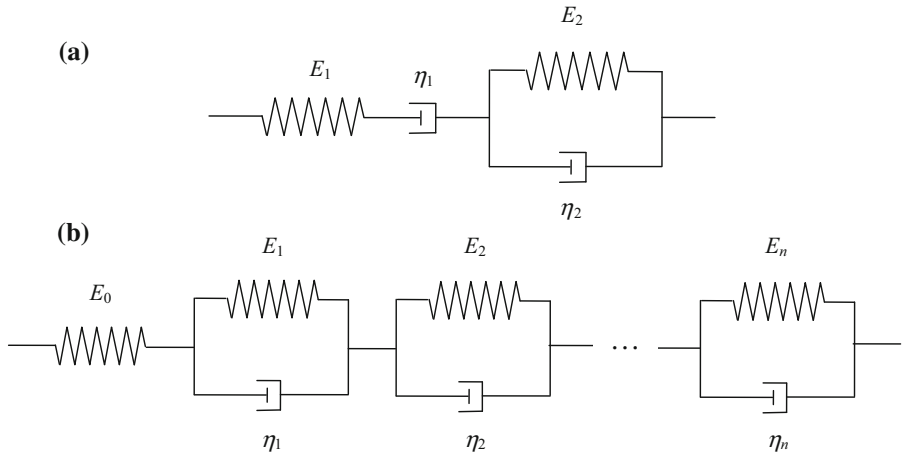

Fig. 2 Burger model (**a**); generalized Kelvin–Voigt model (**b**)

$$D(t) = \frac{1}{E_0} + \sum_{k=1}^{n} \frac{1}{E_k}\left[1 - exp(-t/\bar{t}_k)\right] \quad (8)$$

Equation (8) can be easily written in the form of a Prony series. Indeed, there are several problems related to such a model. Firstly, the physical meaning of all the elements is not always clear. Secondly, fitting an experimental curve by a Prony series is not a trivial task since several restrictions must be imposed (e.g. coefficients have to be positive [6]). The resulting fitting algorithm consists of a constrained least squares problem and sophisticated numerical methods must be implemented (e.g. [45, 46]).

3 Fractional models

Fractional generalization of the models presented in Sect. 2.1 can be obtained by replacing first-order derivatives with derivatives of order $\alpha \in (0,1)$ [24]. According to Caputo's definition, the α-derivative of a generic function f can be expressed in the form:

$$\frac{\mathrm{d}^{\alpha} f(x)}{\mathrm{d}x^{\alpha}} = \frac{1}{\Gamma(1-\alpha)} \int_0^x \frac{f'(y)}{(x-y)^{\alpha}} \mathrm{d}y \quad \alpha \in (0,1) \quad (9)$$

where Γ is the Euler-Gamma function.

According to Eq. (9), function f is obtained for $\alpha = 0$, while the first order classical derivative corresponds to $\alpha = 1$(being $\Gamma(0) = \infty$ and $\Gamma(1) = 1$).

It should be noticed that different definitions of fractional derivative have been proposed in literature [35]. For systems at rest at $t = 0$, Eq. (9) coincides with that provided by Riemann and Liouville, thus proving that the same notation is coherent with both definitions with no loss of generality. A different notation was adopted in [14, 44], where fractional elements were obtained by substituting both springs and dashpots with springpots.

3.1 Scott-Blair element

Replacement of the first-order derivative with the derivative of order $\alpha \in (0,1)$ is equivalent, from a practical point of view, to the substitution of a dashpot with a fractional dashpot (or *springpot*) of order α, which represents the simplest fractional element (also known as Scott-Blair element) (Fig. 3a). The corresponding constitutive equation is ($\alpha \in (0,1)$):

$$\sigma(t) = b_1 \frac{\mathrm{d}^{\alpha} \varepsilon(t)}{\mathrm{d}t^{\alpha}} \quad (10)$$

Equation (10) coincides with Eq. (1) (i.e., the spring case) for $\alpha = 0$, while it leads to Eq. (2) (i.e., the dashpot case) for $\alpha = 1$. As α varies, the physical meaning of parameter b_1 obviously changes (as well as its physical dimensions), passing from a stiffness ($\alpha = 0$) to a viscosity ($\alpha = 1$).

When a creep-based formulation is used for the Scott-Blair element, creep compliance $D(t)$ assumes the following power-law form:

$$D(t) = \frac{t^{\alpha}}{b_1 \Gamma(1+\alpha)} \quad (11)$$

3.2 Double Scott-Blair element

If two springpots in series are considered, a double Scott-Blair element is originated (Fig. 3b). The constitutive relationship can be expressed as ($\alpha, \beta \in (0,1)$):

$$\frac{\mathrm{d}\varepsilon(t)}{\mathrm{d}t} = \frac{1}{b_1} \frac{\mathrm{d}^{1-\alpha}\sigma(t)}{\mathrm{d}t^{1-\alpha}} + \frac{1}{b_2} \frac{\mathrm{d}^{1-\beta}\sigma(t)}{\mathrm{d}t^{1-\beta}} \quad (12)$$

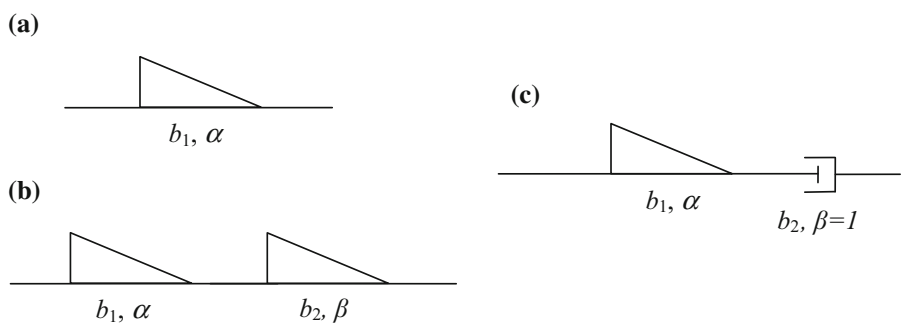

Fig. 3 Scott-Blair model or springpot (**a**); double Scott-Blair model (**b**); proposed model (**c**)

whereas the creep function $D(t)$ is:

$$D(t) = \frac{t^{\alpha}}{b_1\Gamma(1+\alpha)} + \frac{t^{\beta}}{b_2\Gamma(1+\beta)} \quad (13)$$

While considering limit cases, the model described by Eqs. (12–13) yields:

- A single spring (Eq. (1)) with stiffness $b_1b_2/(b_1 + b_2)$ for $\alpha = \beta = 0$.
- A single dashpot (Eq. (2)) with viscosity $b_1b_2/(b_1 + b_2)$ for $\alpha = \beta = 1$.
- The classical Maxwell model (Eq. (4)) for $\alpha = 1$, $\beta = 0$, $\alpha = 0$, $\beta = 1$.
- A single springpot for $\alpha = \beta \neq 0, 1$ described by the two constants $b_1b_2/(b_1 + b_2)$, α.

It can be observed that for $\beta = 1$ the second springpot becomes a dashpot (Fig. 3c): this three-parameter model is adopted in Sect. 4.2 to describe creep-recovery curves obtained from experimental tests.

Interested readers can refer to [24, 44] for a deeper insight on more complex fractional viscoelastic models. In general it is observed that substitution of a dashpot with a springpot involves the introduction of an additional parameter in the analysis. For example, fractionalization of the abovementioned Burger model (Fig. 2a) involves a total of six parameters.

4 Proposed model and experimental validation

As already observed in Sect. 1, many experimental tests on viscoelastic materials reveal a power-law behavior under creep loading. From the point of view of classical rheology, this implies the implementation of the generalized Kelvin–Voigt model with all the related drawbacks discussed in Sect. 2.2. Fractional models discussed in Sect. 3 are much easier to handle, since power-law creep compliance derives directly from the constitutive law (Eqs. (10)–(13)). The book by Mainardi [24] describes in detail all the fractional rheological approaches presented so far in different research fields.

Modelling is certainly more challenging when considering the experimental behavior of viscoelastic materials subjected to both loading and unloading conditions. This is the case of the so called creep-recovery tests, which consist in a first phase, in which a given load is applied to a specimen for a predefined time interval, followed by a second phase, in which the load is removed. During such tests, evolution of strain as a function of time is monitored, thus leading to the direct assessment of its reversible and irreversible components.

Creep-recovery tests are used in the laboratory performance-related characterization of bituminous binders and mixtures in order to evaluate their anti-rutting potential [3, 19, 28, 38]. Such a task is of premium importance since rutting, which results from the accumulation of permanent deformation produced by repeated axle loads, represents one of the main distress types affecting road pavements. Presence of ruts on pavement surfaces leads to a low level of comfort and safety, thus contributing to the decrease of overall road serviceability.

The single springpot element (Fig. 3a) was employed in [9] to model data from creep-recovery compression tests carried out on bituminous mixtures in different temperature conditions. The two parameters (b_1, α) were obtained from fitting which was performed by using the Mathematica® software. However, it was observed that for long loading times fitted recovery strains deviate significantly from recorded data and that implementation of the single springpot element is not adequate to capture the presence of permanent strains. This limitation is clearly described by the following equation, derived from Eq. (11):

$$\varepsilon(t) = \frac{[t^{\alpha}U(t) - (t-t^*)^{\alpha}U(t-t^*)]}{b_1\Gamma(1+\alpha)}\sigma_0 \quad (14)$$

which shows that for such a model strain tends to zero for times t tending to infinite. In Eq. (14) the function $U(t)$ represents the unit step function, while t^* is the starting unloading instant.

Thus, an approach based on two different groups of parameters, one for the loading phase and one for the unloading phase, was proposed. This choice, which leads to a four-coefficient model, is arbitrary and lacks a precise physical meaning.

In order to overcome these drawbacks, a new model consisting of a springpot in series with a dashpot (Fig. 3c) is proposed in this paper to approximate the whole creep-recovery behavior. As observed in Sect. 3.2, such a model represents a particular case of the double Scott-Blair element (Fig. 3b) obtained by

setting $\beta = 1$. The choice of adding a dashpot in series to a springpot is justified by the need of obtaining a non-zero permanent strain at the end of recovery. Starting from Eq. (14) and setting $\beta = 1$, the constitutive law becomes:

$$\varepsilon(t) = \left\{ \left[\frac{t^{\alpha}}{b_1 \Gamma(1+\alpha)} + \frac{t}{b_2} \right] U(t) - \left[\frac{(t-t^*)^{\alpha}}{b_1 \Gamma(1+\alpha)} + \frac{(t-t^*)}{b_2} \right] U(t-t^*) \right\} \sigma_0 \tag{15}$$

In order to validate the model, several shear creep-recovery tests were carried out at various temperatures on two different modified bituminous binders. The test procedure is described in Sect. 4.1, while the comparison between experimental data and theoretical results is discussed in Sect. 4.2.

It should be mentioned that the adopted fractional approach lies in a framework in which non-linear effects are not taken into account or discussed. Nevertheless, since these aspects could be relevant for future applications [11, 25], it may be useful for the reader to briefly synthesize the most important studies developed in this field so far. A detailed reference list can be found in the work by Schapery [43].

Schapery's non-linear viscoelastic theory [20, 40] was derived by using principles of irreversible thermodynamics. In the case of uniaxial loading, if strain is assumed as the independent state variable, the theory leads to a single integral expression, where non-linear stress-dependent terms are related to Gibb's free energy and can be calibrated by specifying a creep compliance function [20]. Furthermore, for low stresses, strain reduces to a power-law function of time, which is linear with respect to applied stress. As already outlined, this can be achieved also by assuming a constitutive law of fractional type.

More recently, Lai and Bakker [17] successfully applied the theory to uniaxial loading of a semi-crystalline polymer, high-density polyethylene. Total strain was assumed to be decomposed into its recoverable visco-elastic and irrecoverable plastic portions, the former being represented by Schapery's thermodynamic theory, the latter being accumulated during loading history. This viscoplastic strain formulation, as well as some work of others on various polymers and composites, were later discussed by Schapery [41], who then generalized his theory to properly take damage and viscoplastic effects into account [42]. Starting from the models presented above, many applications were developed in different research fields [34, 36, 47–49].

Eventually, even in the framework of fractional calculus, non-linear analyses have been discussed both in [33] and [11].

4.1 Materials and test procedure

Materials used in the experimental investigation included a polymer-modified binder (PMB) and an asphalt rubber (AR). Both binders were evaluated in short-term aged conditions after being subjected to the Rolling Thin Film Oven Test (RTFOT) in accordance with AASHTO T240-2009.

PMB was originated from a base bitumen by adding a high percentage of styrene–butadiene–styrene (SBS) according to the undisclosed processing scheme adopted by the plant which provided the material. Modification of bitumen by means of SBS polymers may provide a significant enhancement of its visco-elastic properties [10, 16]. For this reason, the use of SBS polymer-modified bituminous binders is suitable for heavy-duty pavements subjected to high traffic volumes with a significant percentage of heavy and slow-moving vehicles.

AR was a commercially available product containing approximately 18 % crumb rubber (by weight of total binder) derived from the grinding of end-of-life tires. The use of crumb rubber in road paving applications has been known since the 1960s [26] and represents an attractive design option since it allows to solve a serious waste management problem and can simultaneously lead to a significant improvement of pavement performance. In particular, due to their enhanced stiffness and elasticity, crumb rubber modified binders are expected to reduce the accumulation of permanent deformation, thus contributing to the prevention of rut formation [15, 18, 29].

Equipment used for testing was a Physica MCR 302 Dynamic Shear Rheometer (DSR) from Anton Paar Inc., an air bearing stress-controlled device equipped with a permanent magnet synchronous drive (minimum torque = 0.1 μNm, torque resolution <0.1 μNm) and an optical incremental encoder for measurement of angular rotation (resolution <1 μrad). The 25 mm

parallel plates geometry was employed, with a gap between the plates set at 1.0 mm in the case of PMB and 1.5 mm in the case of AR.

Rheological measurements consisted in shear creep-recovery tests carried out at four temperatures (ranging from 58 to 76 °C, with 6 °C increments) at a single stress level (equal to 100 Pa). Duration of creep and recovery phases was set in order to allow materials to reach steady-state flow conditions under loading and to recover most of the delayed elastic deformation after load removal. As indicated in Table 1, this approach led to very long creep and recovery times which were however coherent with those adopted in previous investigations carried out on similar highly modified binders [38, 39]. Two replicates were run for each material-temperature combination and average data were considered in the analysis.

4.2 Results and discussion

The three parameters (α, b_1, b_2) of Eq. (15) were determined by means of a numerical algorithm which allows calculation of the coefficients of a nonlinear regression function by using a least squares estimate. Data recorded in the first 1 % of the loading history were not considered in the analysis, since they may be affected by inaccuracies due to initial settlements of test specimens under loading and to inertia phenomena of the test setup.

Obtained values of (α, b_1, b_2) are reported in Table 2. It can be noticed that α monotonically decreases as a function of increasing temperature T, i.e., when a more viscous behavior is expected. At first glance, this trend might appear misleading, since for α tending to zero the springpot approaches the behavior of a spring. However, it must also be observed that b_1 decreases with temperature, indicating a progressive reduction of springpot resistance to shear deformation.

Table 1 Test conditions adopted in the experimental investigation

Temperature (°C)	Shear stress level (Pa)	Creep time (s)	Recovery time (s)
58	100	10,800	43,200
64	100	1,800	21,600
70	100	600	10,800
76	100	300	7,200

Table 2 Fitted parameters (α, b_1, b_2) for creep-recovery tests carried out at different temperatures

T (°C)	PMB			AR		
	α	b_1 (s^{α} N/m^2)	b_2 (s N/m^2)	α	b_1 (s^{α} N/m^2)	b_2 (s N/m^2)
58	0.611	0.555	9.26	0.461	0.909	15.7
64	0.571	0.312	1.88	0.372	0.476	6.02
70	0.549	0.213	0.758	0.359	0.345	2.47
76	0.502	0.154	0.215	0.341	0.256	1.08

In other terms, as a result of the combined effects of α and b_1 variations, as temperature increases and coherently with expectations, the relative contribution of the springpot to overall deformation becomes smaller than that of the dashpot. As expected, parameter b_2, representing viscosity of the dashpot, also decreases with temperature.

By comparing results obtained for the two binders, it can be observed that at any given temperature AR exhibits lower values of α, higher values of b_1 and higher values of b_2 than PMB. Coherently with the composition of the considered materials, this indicates that AR has a more pronounced elastic behavior and a higher stiffness than PMB.

Experimental data were compared with those obtained by using Eq. (15) with fitted parameters (Table 2). Results referring to different temperatures for PMB are reported in Figs. 4 and 5a, b, while Figs. 4 and 5c, d display the percent relative error δ of each case. Indeed, a fairly good agreement is generally found. In the creep phase, δ remains always below 10 %, with maximum values (nearly 8 %) observed at $T = 58$ and 76 °C, i.e. in the least and most viscous cases, respectively. During recovery, δ does not exceed 3 %, showing a monotonic trend with time. Similar considerations hold for tests carried out on AR (Figs. 6, 7): theoretical results seem to be accurate both during the creep phase (with maximum errors, close to 7 %, occurring once again for the extremes cases corresponding to $T = 58$ and 76 °C) and during recovery (δ being always less than 5 %).

In order to verify the capability of the model to predict material response under different test conditions, shear strain values calculated by implementing the proposed model were compared with available experimental data not used in the calibration process. These data refer to creep tests carried out on binder

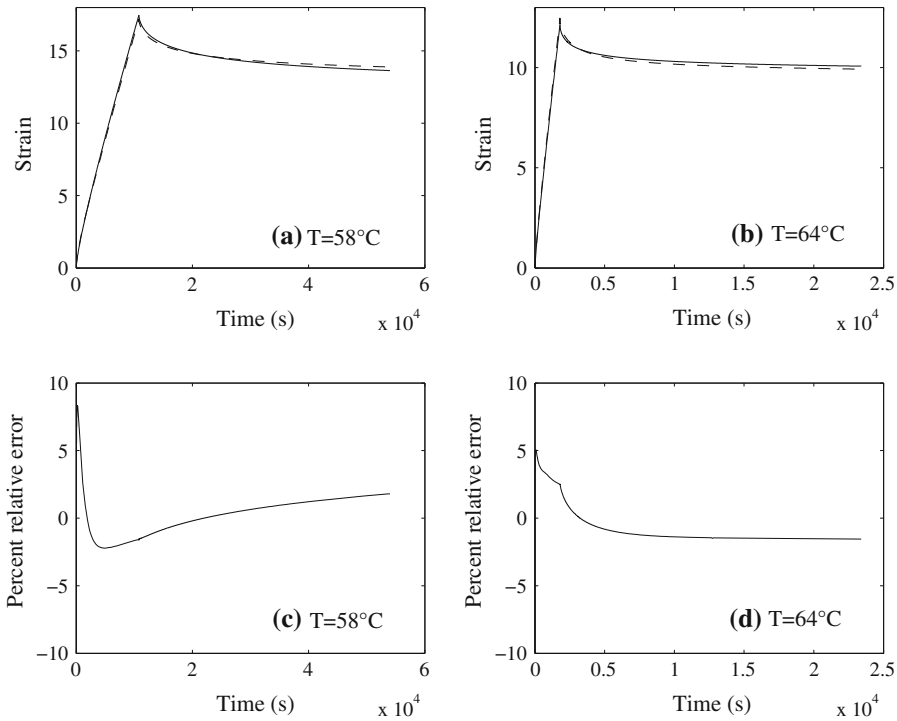

Fig. 4 Creep-recovery tests on binder PMB: **a**, **b** experimental data (*dashed line*) and theoretical results (*solid line*) (**a**: for $T = 58$ °C; **b**: for $T = 64$ °C; **c**, **d** percent relative error (**c**: for $T = 58$ °C; **d**: for $T = 64$ °C)

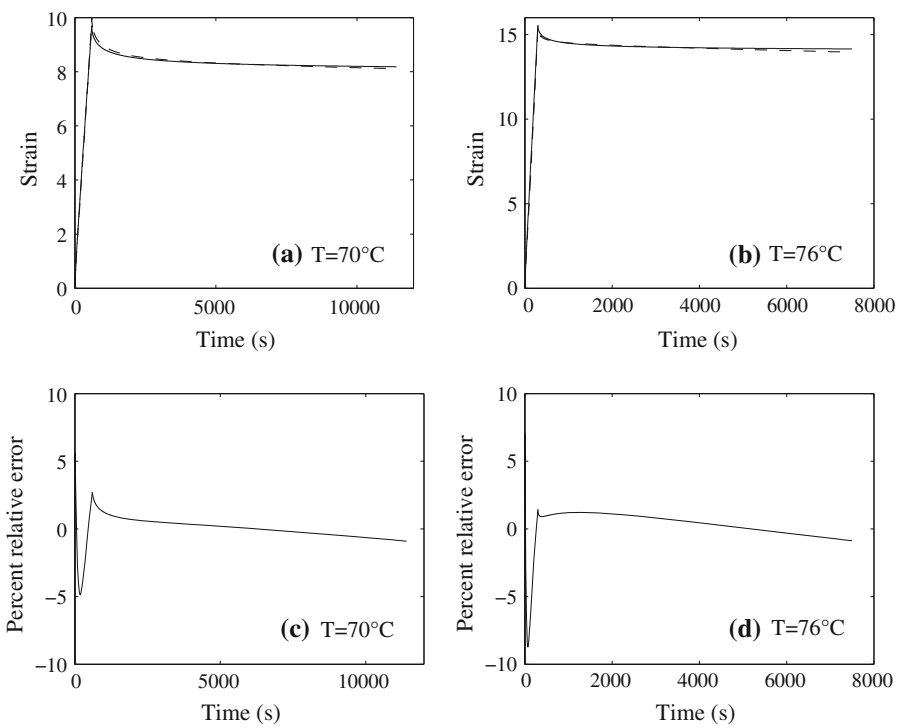

Fig. 5 Creep-recovery tests on binder PMB: **a**, **b** experimental data (*dashed line*) and theoretical results (*solid line*) (**a**: for $T = 70$ °C; **b**: for $T = 76$ °C; **c**, **d** percent relative error (**c**: for $T = 70$ °C; **d**: for $T = 76$ °C)

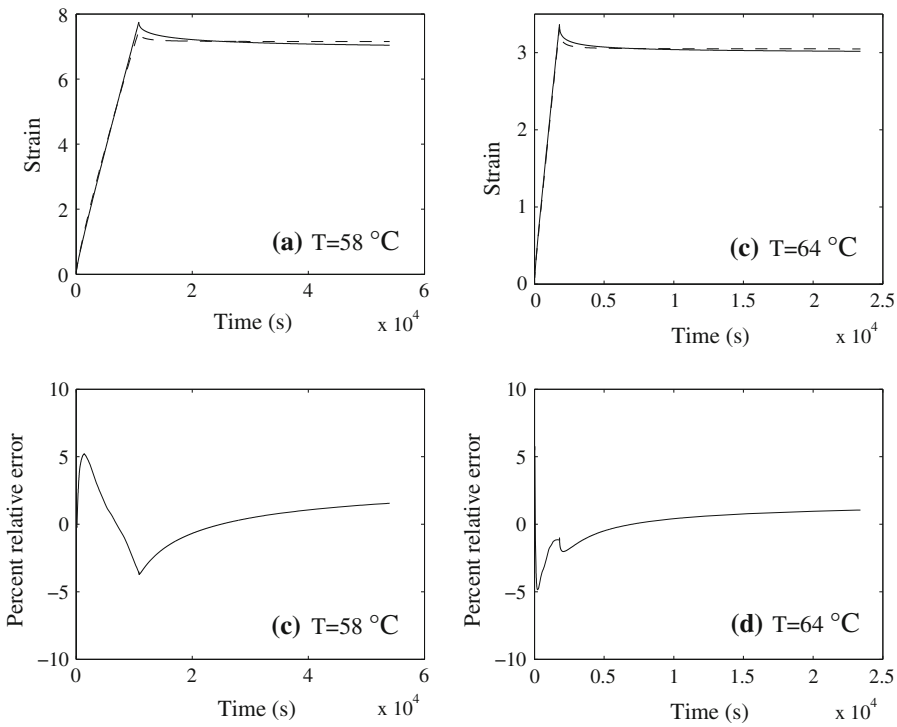

Fig. 6 Creep-recovery tests on binder AR: **a**, **b** experimental data (*dashed line*) and theoretical results (*solid line*) (**a**: for $T = 58$ °C; b: for $T = 64$ °C; **c**, **d** percent relative error (**c**: for $T = 58$ °C; **d**: for $T = 64$ °C)

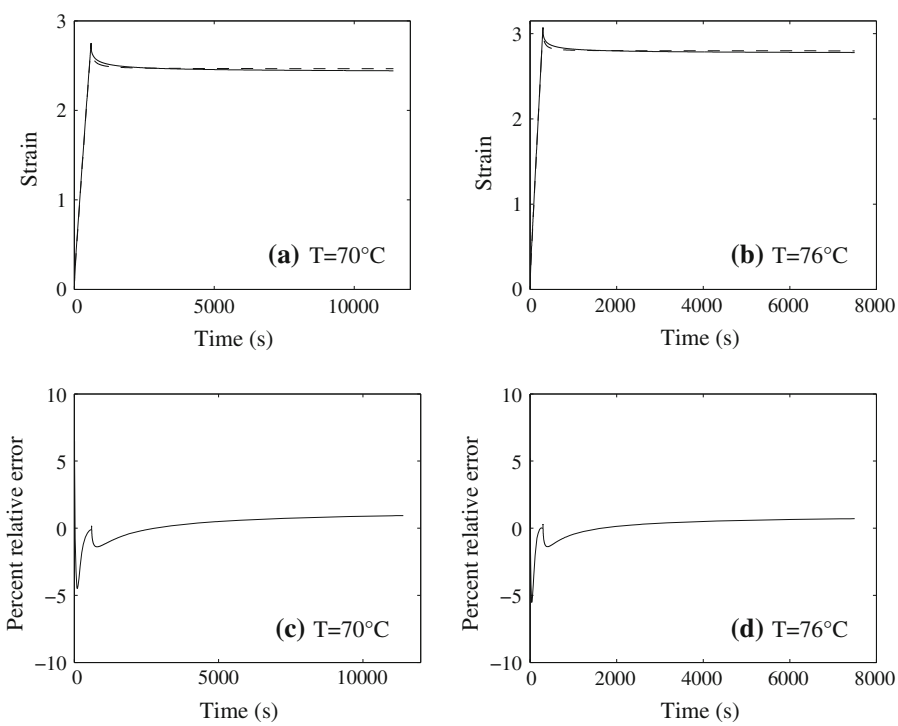

Fig. 7 Creep-recovery tests on binder AR: **a**, **b** experimental data (*dashed line*) and theoretical results (*solid line*) (**a**: for $T = 70$ °C; **b**: for $T = 76$ °C; **c**, **d** percent relative error (**c**: for $T = 70$ °C; **d**: for $T = 76$ °C)

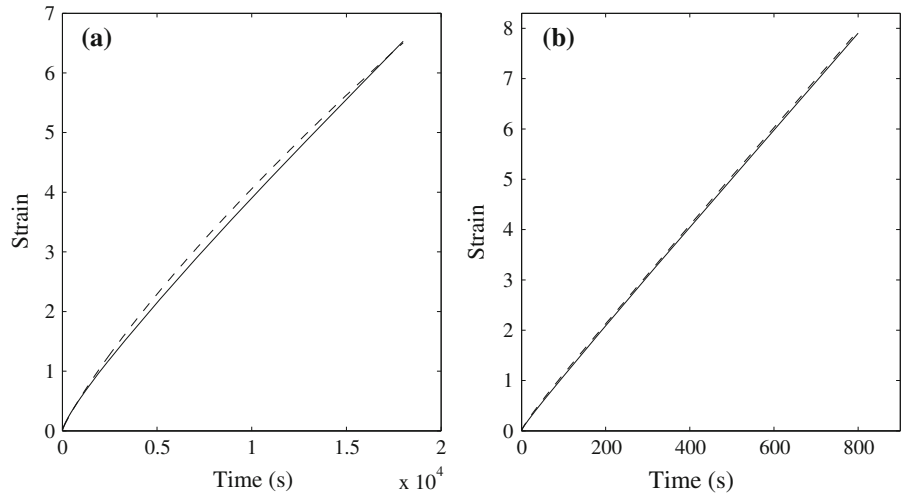

Fig. 8 Creep tests on binder PMB: comparison between experimental data (*dashed line*) and predictions (*solid line*) (**a**: for $T = 58$ °C; **b**: for $T = 76$ °C)

PMB at a lower stress level (20 Pa) and the two extreme temperatures (58 and 76 °C). Theoretical predictions, obtained by using the parameters given in Table 2, and experimental curves are shown in Fig. 8. Matching appears to be satisfactory in both cases with maximum relative deviations lower than 5 %.

5 Conclusions

A fractional model, consisting of a springpot in series with a dashpot, was used in this study to describe the creep-recovery behavior of two different modified bituminous binders (containing SBS polymer and crumb rubber, respectively). Theoretical results matched the experimental data gathered from shear creep-recovery tests carried out at different temperatures. In particular, during the creep phase, absolute percent relative errors were generally lower than 8 %, while during the recovery phase maximum deviations were comprised in the ±5 % range. For one of the two binders, parameter calibration was successfully verified by considering a different data set, obtained from creep tests carried out at a lower loading level. Based on the findings synthesized above, it can be concluded that the proposed fractional model is superior to others adopted for the analysis of bituminous materials for road pavements. In particular, it seems to be more accurate than the single springpot considered in [9] and easier to be implemented than the six-parameter fractional Burger element [33].

Future developments of the study described in this paper will consider three-dimensional characterization, numerical implementation of the model via a FE code and generalization of the approach to take into account non-linear effects [11].

References

1. Atanackovic TM, Pilipovic S, Zorica D (2011) Distributed-order fractional wave equation on a finite domain. Stress relaxation in a rod. Int J Eng Sci 49:175–190
2. Atanackovic TM, Pilipovic S, Zorica D (2013) Forced oscillations of a body attached to a viscoelastic rod of fractional derivative type. Int J Eng Sci 64:54–65
3. Bai F, Yang X, Zeng G (2014) Creep and recovery behavior characterization of asphalt mixture in compression. Constr Build Mater 54:504–511
4. Barpi F, Valente S (2003) Creep and fracture in concrete: a fractional order rate approach. Eng Fract Mech 70:611–623
5. Barpi F, Valente S (2004) A fractional order rate approach for modeling concrete structures subjected to creep and fracture. Int J Solids Struct 41:2607–2621
6. Bradshaw RD, Brinson LC (1997) A sign control method for fitting and interconverting material functions for linearly viscoelastic. Solids Mech Time-Depend Mater 1:85–108
7. Caputo M, Mainardi F (1971) Linear models of dissipation in anelastic solids. Nuovo Cimento 1:161–198
8. Carpinteri A, Mainardi F (1997) Fractals and fractional calculus in continuum mechanics. Springer-Verlag, Wien
9. Celauro C, Fecarotti C, Pirrotta A, Collop A (2012) Experimental validation of a fractional model for creep/recovery testing of asphalt mixtures. Constr Build Mater 36:458–466
10. Collins JH, Bouldin MG, Gelles R, Berker A (1991) Improved performance of paving asphalts by polymer modification. J Assoc Asphalt Paving Technol 60:43–79

11. Di Mino G, Airey G, Di Paola M, Pinnola F, D'Angelo G, Lo Presti D. Linear and nonlinear fractional hereditary constitutive laws of asphalt mixtures. J Civil Eng Manage. doi:10.3846/13923730.2014.914104
12. Di Paola M, Pirrotta A, Valenza A (2011) Visco-elastic behavior through fractional calculus: an easier method for best fitting experimental results. Mech Mater 43:799–806
13. Di Paola M, Pinnola F, Zingales M (2013) A discrete mechanical model of fractional hereditary materials. Meccanica 48:1573–1586
14. Hilfer R (2000) Fractional calculus in physics. World Scientific Pub Co, Singapore
15. Hsu T, Chen S, Hung K (2011) Performance evaluation of asphalt rubber in porous asphalt-concrete mixtures. J Mater Civil Eng 23:342–349
16. King GN, Muncy HW, Proudhomme JB (1986) Polymer modification: binder's effect on mix properties. J Assoc Asphalt Paving Technol 55:519–540
17. Lai J, Bakker A (1995) An integral constitutive equation for nonlinear plasto-viscoelastic behavior of high density polyethylene. Polym Eng Sci 35:1339–1347
18. Lee S-J, Akisetty CK, Amirkhanian SN (2008) The effect of crumb rubber modifier (CRM) on the performance properties of rubberized binders in HMA pavements. Constr Build Mater 22:1368–1376
19. Levenberg E (2009) Viscoplastic response and modeling of asphalt-aggregate mixes. Mater Struct 42:1139–1151
20. Lou YC, Schapery RA (1971) Viscoelastic characterization of a non-linear fiber-reinforced plastic. J Compos Mater 5:208–234
21. Machado JT, Kiryakova V, Mainardi F (2011) Recent history of fractional calculus. Commun Nonlinear Sci Numer Simul 11:1140–1153
22. Magin RL (2006) Fractional calculus in bioengineering. Begel House Inc, Redding
23. Mainardi F (1994) Fractional relaxation in anelastic solids. J Alloy Compd 211:534–538
24. Mainardi F (2010) Fractional calculus and waves in linear viscoelasticity: an introduction to mathematical models. Imperial College Press, London
25. Masad E, Huang CW, Airey G, Muliana A (2008) Nonlinear viscoelastic analysis of unaged and aged asphalt binders. Constr Build Mater 22:2170–2179
26. McDonald CH (1981) Recollections of early asphalt-rubber history. In: Proceedings of national seminar on asphalt-rubber, San Antonio
27. Meral FC, Royston TJ, Magin R (2009) Fractional calculus in viscoelasticity: an experimental study. Commun Nonlinear Sci Numer Simul 15:939–945
28. Merusi F, Giuliani F (2011) Intrinsic resistance to non-reversible deformation in modified asphalt binders and its relation with specific criteria. Constr Build Mater 25:3356–3366
29. Moreno F, Sol M, Martín J, Pérez M, Rubio MC (2013) The effect of crumb rubber modifier on the resistance of asphalt mixes to plastic deformation. Mater Des 47:274–280
30. Müller S, Kästner M, Brummund J, Ulbricht V (2013) On the numerical handling of fractional viscoelastic material models in a FE analysis. Comput Mech 51:999–1012
31. Nutting PG (1921) A new general law of deformation. J Frankl Inst 191:679–685
32. Nutting PG (1943) A general stress-strain formula. J Frankl Inst 253:513–524
33. Oeser M, Pellin T, Scarpas T, Kasbergen C (2008) Studies on creep and recovery of rheological bodies based upon conventional and fractional formulations and their application on asphalt mixture. Int J Pavement Eng 9:373–386
34. Park SW, Kim R, Schapery RA (1996) A viscoelastic continuum damage model and its application to uniaxial behavior of asphalt concrete. Mech Mater 24:241–255
35. Podlubny I (1999) Fractional differential equations. Academic Press, San Diego
36. Provenzano PP, Lakes RS, Corr DT, Vanderby R Jr (2002) Application of nonlinear viscoelastic models to describe ligament behaviour. Biomech Model Mechanobiol 1:45–57
37. Samko G, Kilbas AA, Marichev OI (1993) Fractional integrals and derivatives. Gordon and Breach, Amsterdam
38. Santagata E, Baglieri O, Dalmazzo D, Tsantilis L (2013) Evaluation of the anti-rutting potential of polymer modified binders by means of creep-recovery tests shear tests. Mater Struct 46:1673–1682
39. Santagata E, Baglieri O, Alam M, Dalmazzo D (2014) A novel procedure for the evaluation of anti-rutting potential of asphalt binders. Int J Pavement Eng. doi:10.1080/10298436.2014.942859
40. Schapery RA (1969) On the characterization of non-linear viscoelastic materials. Polym Eng Sci 9:295–310
41. Schapery RA (1997) Nonlinear viscoelastic and viscoplastic constitutive equations based on thermodynamics. Mech Time-Depend Mater 1:209–240
42. Schapery RA (1999) Nonlinear viscoelastic and viscoplastic constitutive equations with growing damage. Int J Fract 97:33–66
43. Schapery RA (2000) Nonlinear viscoelastic solids. Int J Solids Struct 37:359–366
44. Schiessel H, Metzler HR, Blumen A, Nonnenmacher TF (1995) Generalized viscoelastic models: their fractional equations with solutions. J Phys A: Math Theor 28:6567–6584
45. Sorvari J, Malinen M (2007) On the direct estimation of creep and relaxation functions. Mech Time-Depend Mater 11:143–157
46. Tschoegl NW (1989) The phenomenological theory of linear viscoelastic behavior: an introduction. Springer, Berlin
47. Uzan J (1996) Asphalt concrete characterization for pavement performance prediction. J Assoc Asphalt Paving Technol 65:573–607
48. Uzan J, Perl M, Sides A (1986) Numerical simulation of fatigue creep crack growth in a visco-elastoplastic material, II: experimental validation and application. Eng Fract Mech 23:333–344
49. Ye Y, Yang X, Chen C (2010) Modified Schapery's model for asphalt sand. J Eng Mech 136:448–454